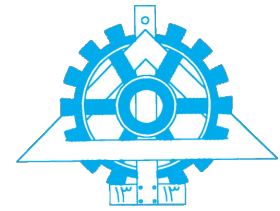




University of Tehran
College of Engineering
School of Electrical & Computer Eng



Principles of Cognitive Science

Assignment 3 EEG

Name

Reza Chehreghani

Student ID

810101401

August 6, 2025

Contents

1 Preprocessing	1
1.1 Importing Data and Events	2
1.2 Scaling to Microvolts	2
1.3 Downsampling	3
1.4 High-Pass Filtering	3
1.5 Importing Channel Locations	4
1.6 Removing Line Noise	5
1.7 Rejecting Bad Channels	6
1.8 Interpolating Removed Channels	7
1.9 Re-referencing the Data	7
1.10 Removing Bad Segments	7
1.11 Re-referencing Again	7
1.12 Running AMICA and ICLabel	7
1.13 Epoching and Baseline Correction	9
2 Event-Related Potential (ERP)	9
2.1 Permutation Test Results	11
2.2 Cluster-Based Permutation Test Results	13
3 Time-Frequency Analysis	14
4 Multivariate Pattern Analysis (MVPA)	19
4.1 Temporal MVPA	19
4.2 Spatial MVPA	21
4.3 Cross-Temporal Generalization	21

5 Representational Dissimilarity Matrices (RDM) and Representational Similarity Analysis (RSA)

24

List of Figures

1	Data scale before conversion (in volts)	2
2	Data scale after conversion to microvolts.	3
3	Amplitude and phase response of the 1 Hz high-pass filter.	4
4	2D scalp topography of the EEG channels.	5
5	3D scalp topography of the EEG channels.	5
6	Power spectrum before line noise removal.	6
7	Power spectrum after CleanLine processing.	6
8	Component labels generated by ICLabel for one subject.	8
9	Topography of a component likely corresponding to occipital brain activity. .	9
10	ERPs across all channels for face and dollhouse trials.	10
11	ERP comparison for face vs. dollhouse trials in channels O1, O2, and Oz. .	10
12	Permutation test showing a significant negative cluster (N170) in channel T8. .	11
13	Permutation test showing a significant positive cluster (P300) in channel P4. .	12
14	Cluster-based test confirming a significant N170 component at T8.	13
15	Cluster-based test confirming significant P300 components at P4.	13
16	Time-frequency maps (ERSPs) for all channels, plotted separately for face and dollhouse stimuli.	15
17	ERSP in channel O1: face vs. dollhouse.	15
18	ERSP in channel PO4: face vs. dollhouse.	16
19	ERSP in channel PO7: face vs. dollhouse.	17
20	ERSP in channel TP9: face vs. dollhouse.	18
21	Temporal decoding accuracy over time.	19
22	Temporal decoding AUC score over time.	20
23	Temporal decoding F1 score over time.	20
24	Topographic map of LDA classifier weights during 100–300 ms.	21
25	Cross-temporal generalization matrix (accuracy).	22

26	Cross-temporal generalization matrix (AUC)	23
27	EEG RDMs over time.	25
28	EEG RDMs across channels.	25
29	RSA over time between EEG and CORnet-S RDMs (V1, V2, V4, IT).	26

Preprocessing

I used EEGLAB for preprocessing the EEG data. The complete pipeline is as follows:

1. Import data and event markers
2. Scale the data to microvolts
3. Downsample to 256 Hz
4. Apply a 1 Hz high-pass filter
5. Import channel location information
6. Remove line noise using the CleanLine extension
7. Reject bad channels
8. Interpolate removed channels
9. Re-reference the data to the average of all channels
10. Remove noisy segments
11. Re-reference again after segment removal
12. Run AMICA with the corrected data rank
13. Epoch the data and apply baseline correction

1.1 Importing Data and Events

For each subject, I imported the provided .mat files using EEGLAB. Each file contained 64 signals: the first 63 channels were EEG channels referenced to Fz, and the last channel encoded the event markers.

1.2 Scaling to Microvolts

The raw EEG data were originally in volts, resulting in very small values (e.g., in the range of 10^{-5}), which caused EEGLAB to incorrectly estimate the data rank as zero. To address this, I multiplied the data by 10^6 to convert it to microvolts.

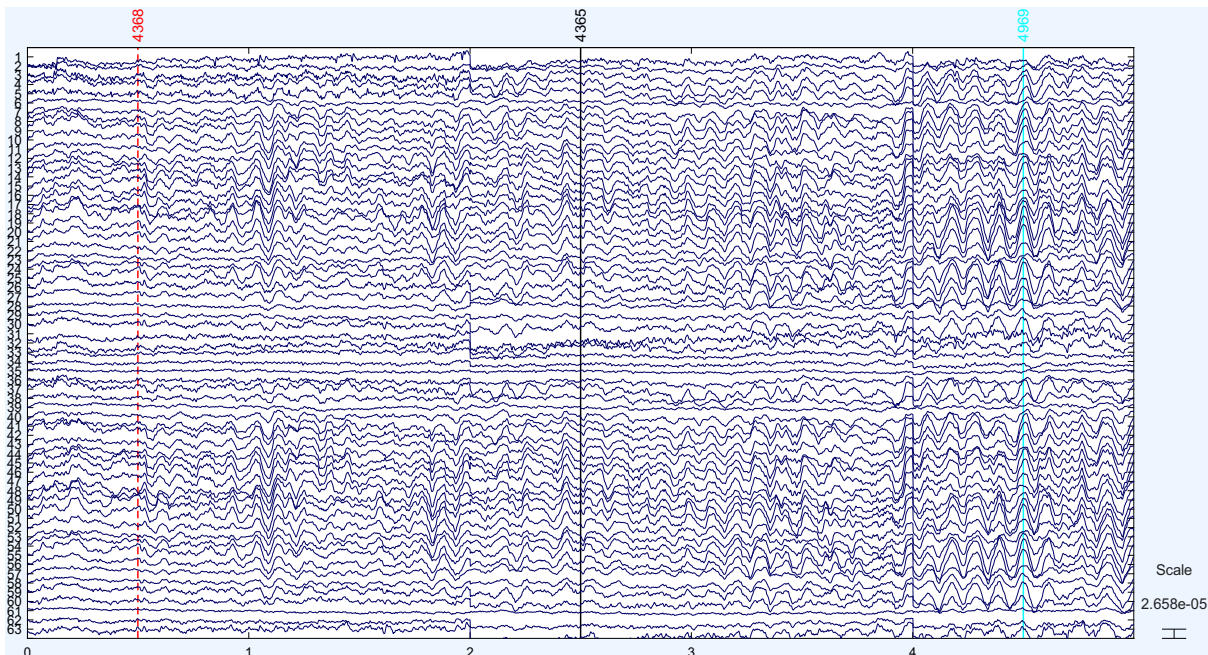


Figure 1: Data scale before conversion (in volts).

As shown above, the EEG values are on the order of $2.658 \times 10^{-5} V$.

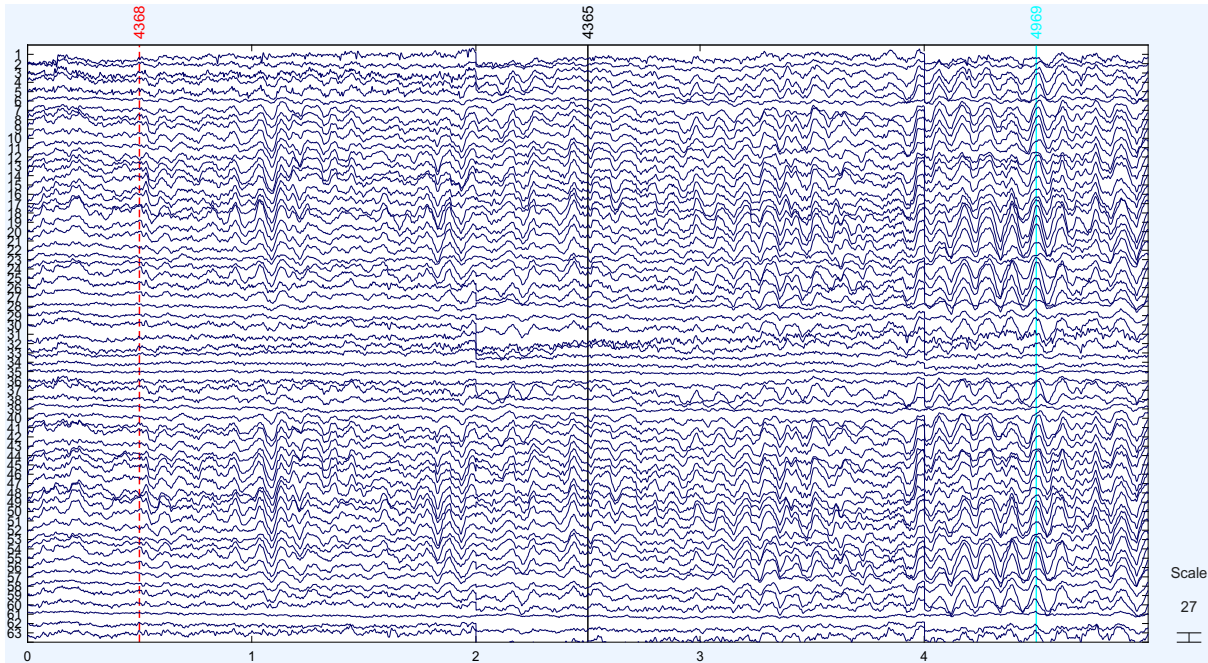


Figure 2: Data scale after conversion to microvolts.

After scaling, the amplitude is approximately $27\mu V$, which is within the expected physiological range.

1.3 Downsampling

To reduce computational cost and maintain sufficient temporal resolution, I downsampled the data to 256 Hz.

1.4 High-Pass Filtering

I applied a 1 Hz high-pass FIR filter to remove slow drifts and baseline shifts from the signal. This step is particularly important for ICA and event-related analyses.

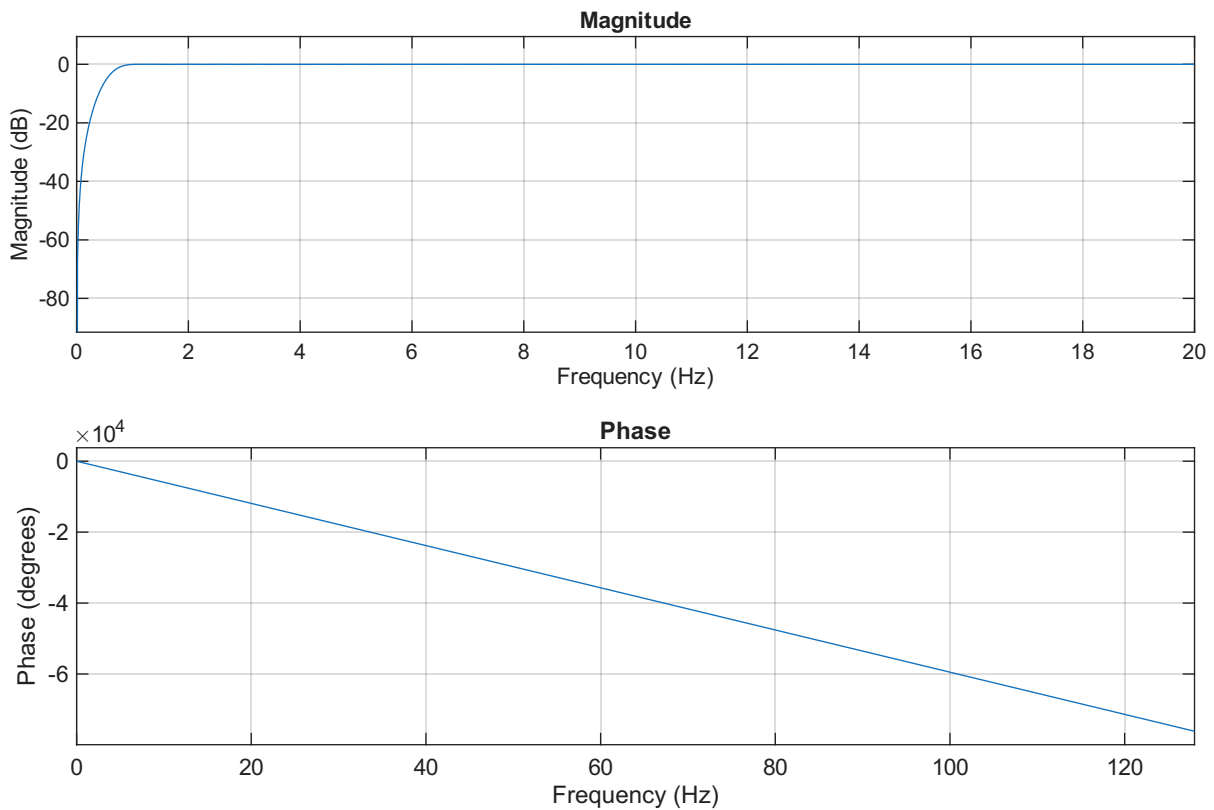


Figure 3: Amplitude and phase response of the 1 Hz high-pass filter.

1.5 Importing Channel Locations

I imported the standard 64-channel location file based on the 10–10 EEG system. Fz was used as the initial reference.

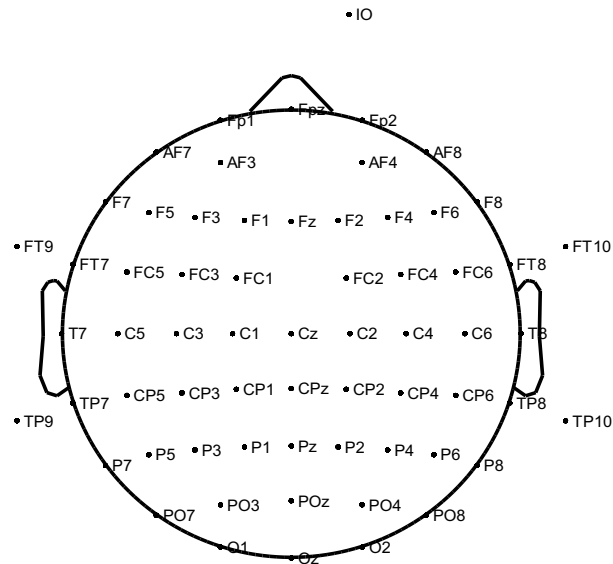


Figure 4: 2D scalp topography of the EEG channels.

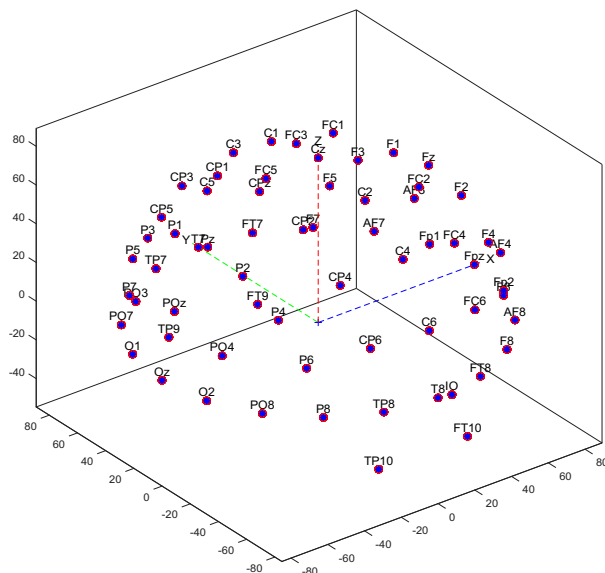


Figure 5: 3D scalp topography of the EEG channels.

1.6 Removing Line Noise

To remove 50 Hz power line interference, I used the CleanLine plugin available in EEGLAB. It adaptively filters narrow-band noise using multi-taper methods.

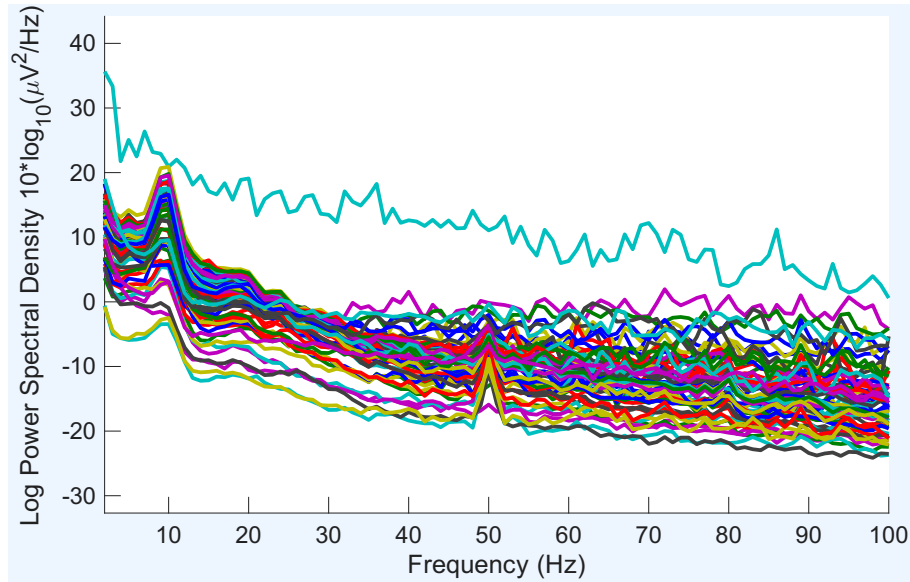


Figure 6: Power spectrum before line noise removal.

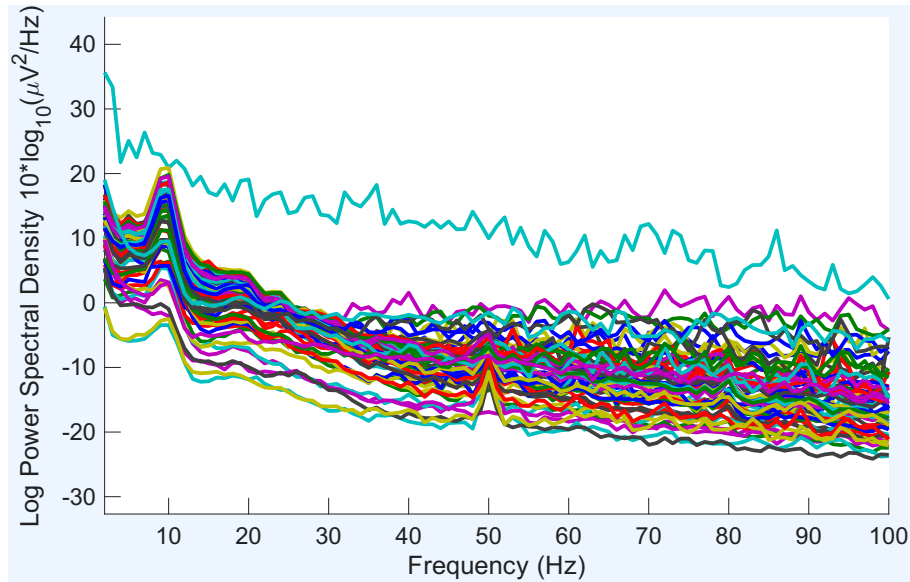


Figure 7: Power spectrum after CleanLine processing.

1.7 Rejecting Bad Channels

By visually inspecting channel time series and spectra, I identified and removed channels with poor signal quality (e.g., flat, disconnected, or overly noisy).

1.8 Interpolating Removed Channels

To preserve the spatial structure of the EEG and avoid ICA biases, I interpolated the previously removed channels using spherical interpolation.

1.9 Re-referencing the Data

I re-referenced the EEG to the average of all channels to remove any bias from a single reference electrode and to ensure a zero-mean scalp potential.

1.10 Removing Bad Segments

Noisy time segments (e.g., containing muscle artifacts or movement) were manually or automatically rejected to improve data quality before ICA.

1.11 Re-referencing Again

After rejecting segments, I re-applied average referencing to restore a zero-mean scalp distribution and prepare the data for ICA decomposition.

1.12 Running AMICA and ICLabel

To separate brain activity from artifacts, I used AMICA, an advanced ICA algorithm. After decomposition, I applied ICLabel to classify each independent component.



Figure 8: Component labels generated by ICLabel for one subject.

I also examined one component classified as brain and verified its scalp distribution.

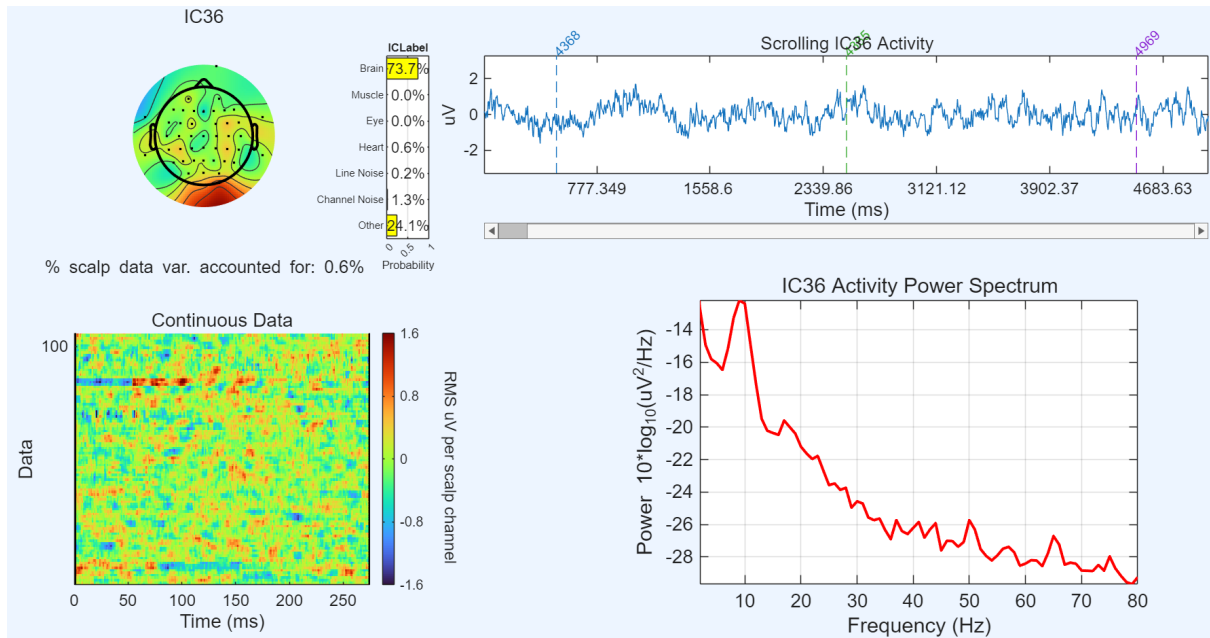


Figure 9: Topography of a component likely corresponding to occipital brain activity.

Based on ICLabel confidence values, I removed components corresponding to eye movements, muscle artifacts, heartbeats, line noise, and channel noise.

1.13 Epoching and Baseline Correction

I epoched the continuous data from -500 ms to $+1500$ ms relative to stimulus onset. Then, I applied baseline correction using the pre-stimulus interval from -500 ms to 0 ms.

Event-Related Potential (ERP)

To compare the neural responses to face and dollhouse stimuli, I separated the trials by stimulus type and computed the ERP for each individual channel. The full-channel ERP plots for both categories are shown below:

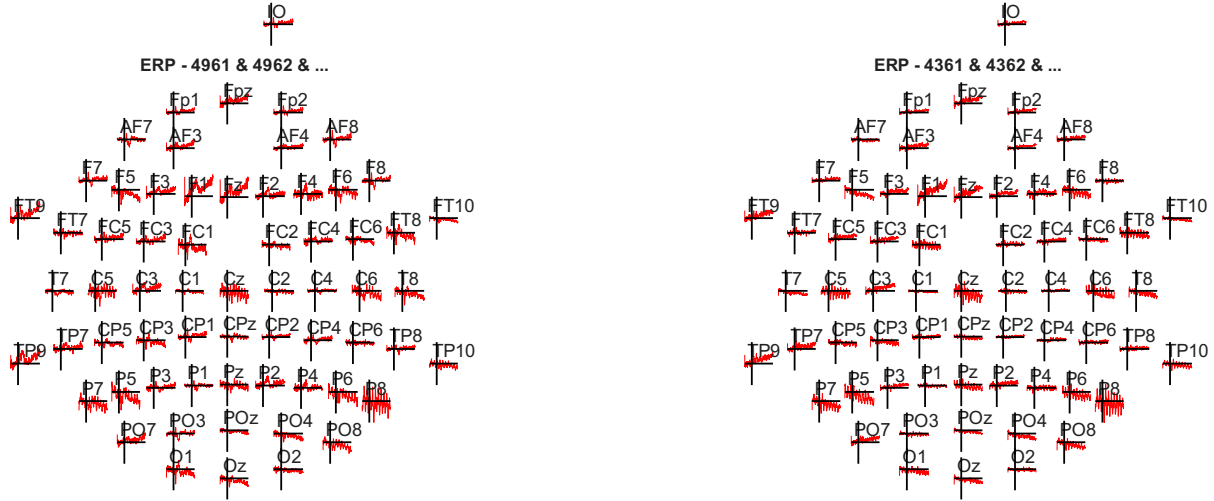


Figure 10: ERPs across all channels for face and dollhouse trials.

To focus on visual processing areas, I examined the ERPs from occipital channels **O1**, **O2**, and **Oz**:

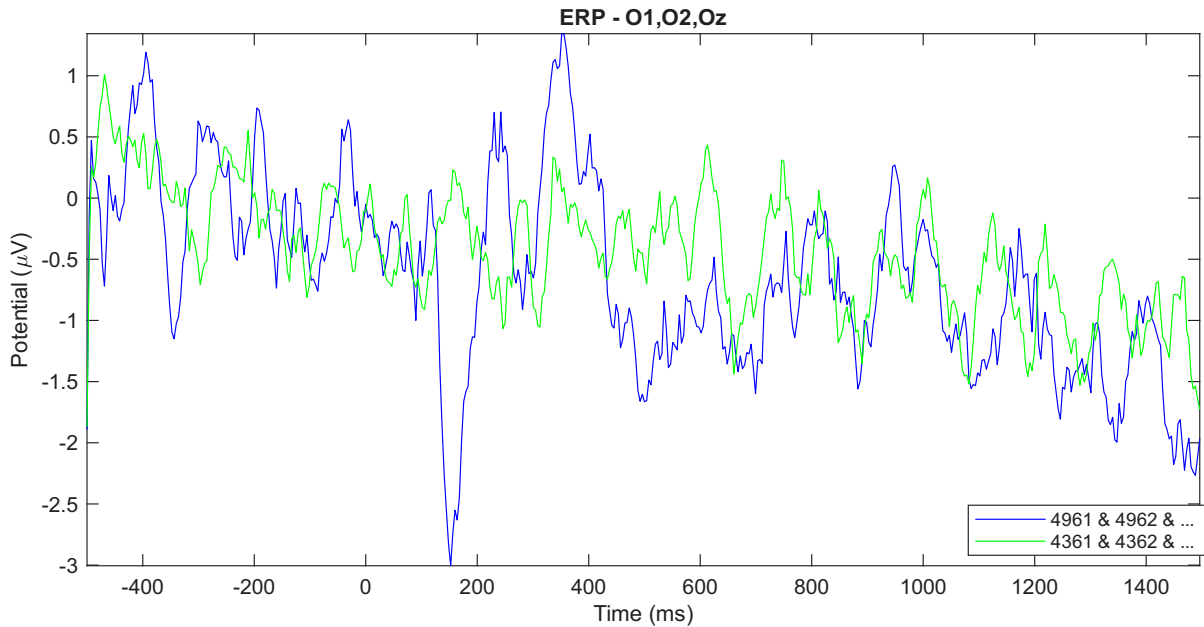


Figure 11: ERP comparison for face vs. dollhouse trials in channels O1, O2, and Oz.

As shown in the figure, the ERP waveform for face stimuli exhibits:

- A prominent **negative peak around 170 ms** (known as the **N170**), which is classically

associated with face perception.

- A clear **positive peak around 300 ms** (interpreted as the **P300**), often linked to attention and stimulus categorization.

To statistically evaluate these differences, I used two approaches:

1. **Permutation tests**
2. **Cluster-based permutation tests** (via FieldTrip integration)

2.1 Permutation Test Results

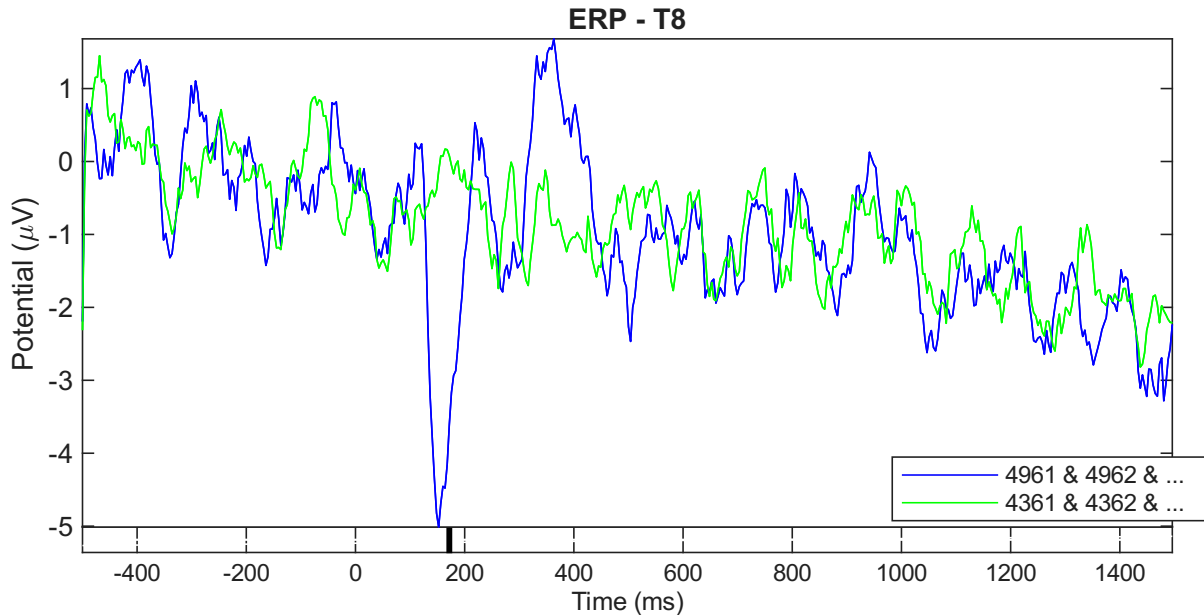


Figure 12: Permutation test showing a significant negative cluster (N170) in channel T8.

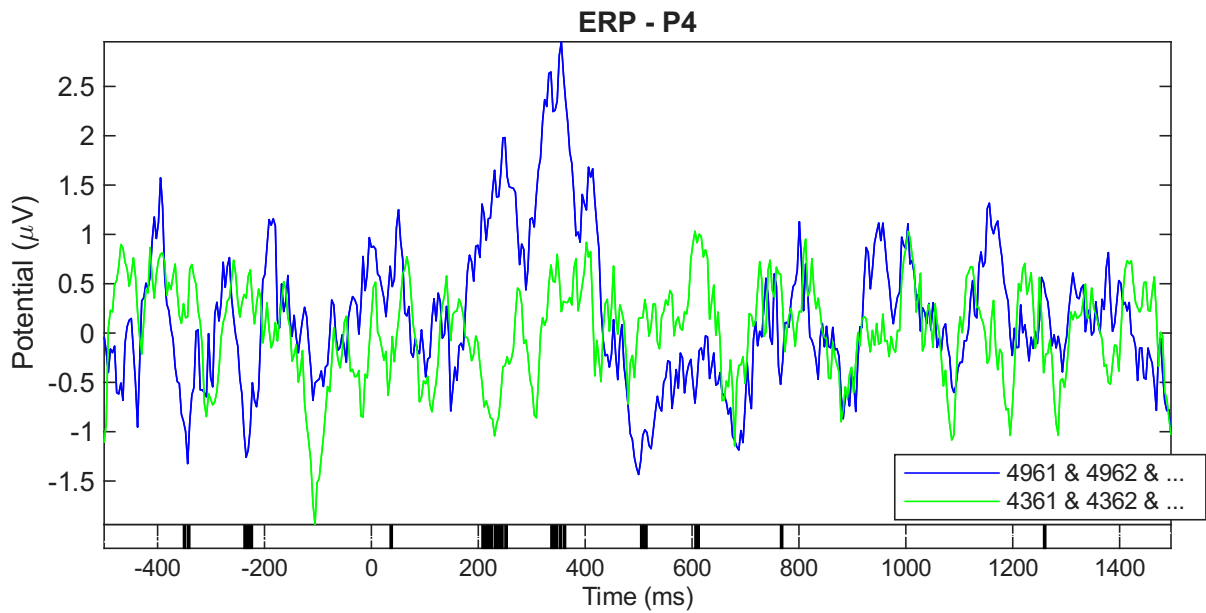


Figure 13: Permutation test showing a significant positive cluster (P300) in channel P4.

These results confirm:

- A **significant N170 component at T8** around 170 ms for face stimuli.
- A **significant P300 component at P4** around 300 ms, stronger for face trials.

2.2 Cluster-Based Permutation Test Results

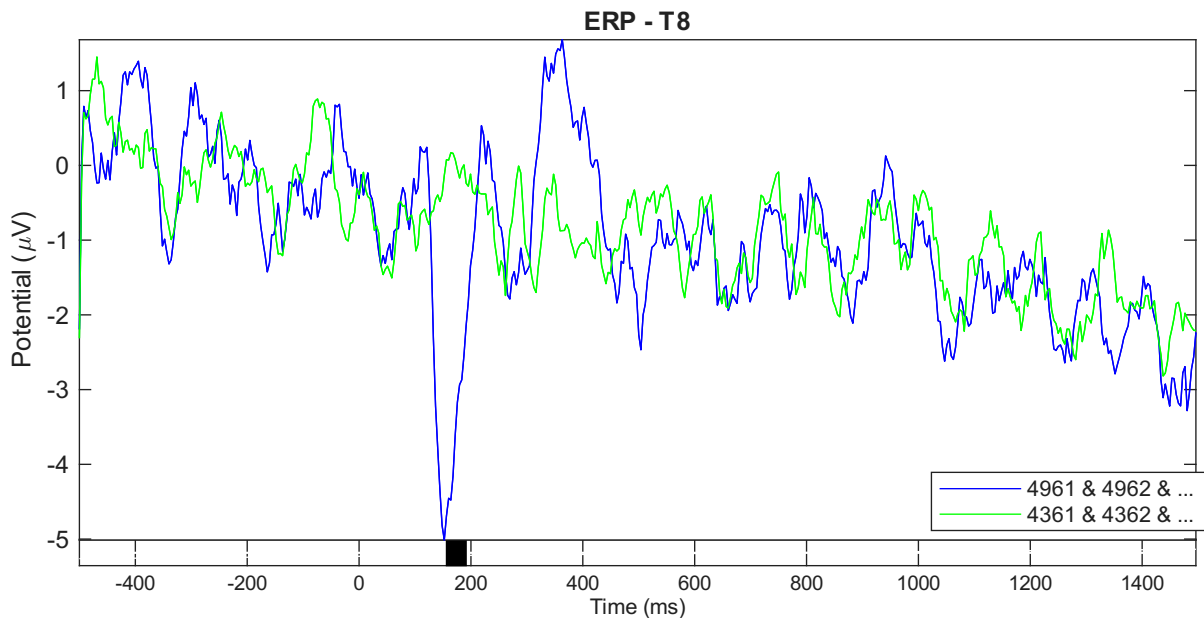


Figure 14: Cluster-based test confirming a significant N170 component at T8.

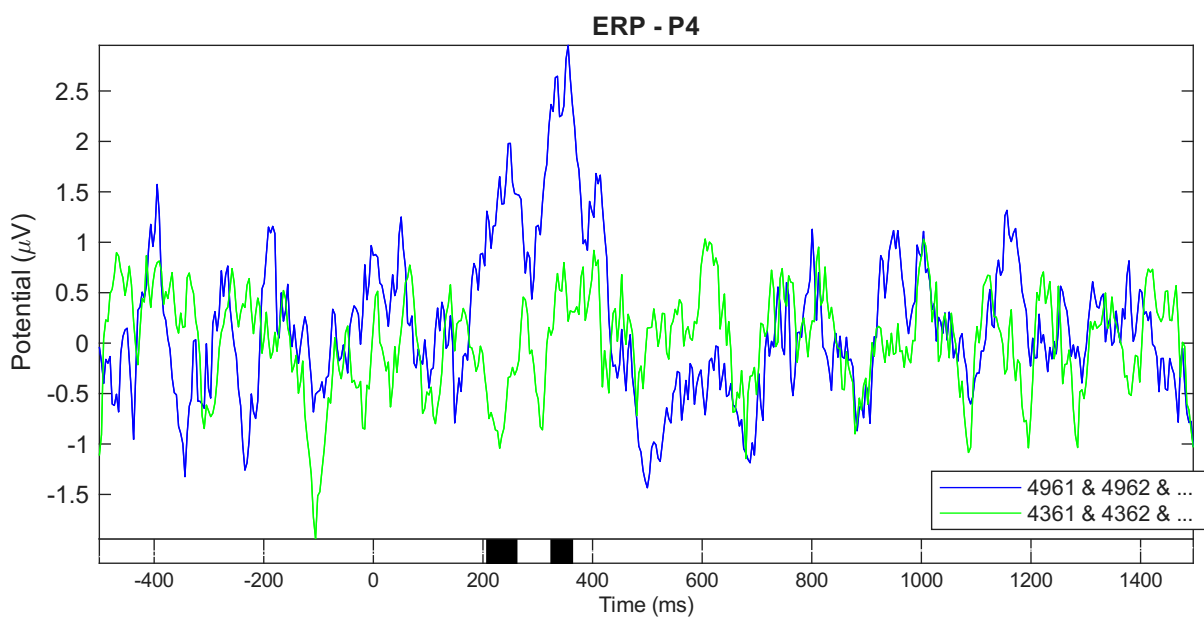


Figure 15: Cluster-based test confirming significant P300 components at P4.

The cluster-based approach further supports the earlier findings:

- The **N170 component** is statistically significant in the **right temporal channel T8**, consistent with right-lateralized face processing.
- The **P300 component** is also significantly larger for face stimuli in **posterior channel P4**.

Interpretation

Together, these results highlight that:

- **Face stimuli evoke stronger early visual responses**, especially the N170, which is known to reflect face-selective neural activity in the visual cortex.
- **Later positive deflections (P300)** suggest greater attentional or categorical processing for face stimuli compared to dollhouses.

These findings are in line with previous ERP literature on face processing and confirm that the EEG signals contain temporally and spatially distinct markers that differentiate face from non-face visual categories.

Time-Frequency Analysis

To investigate the frequency-specific dynamics of neural activity in response to face and dollhouse stimuli, I performed a time-frequency analysis using EEGLAB's ERSP (Event-Related Spectral Perturbation) plots.

ERSPs Across All Channels

The ERSP maps for all channels are shown below, separately for face and dollhouse trials:

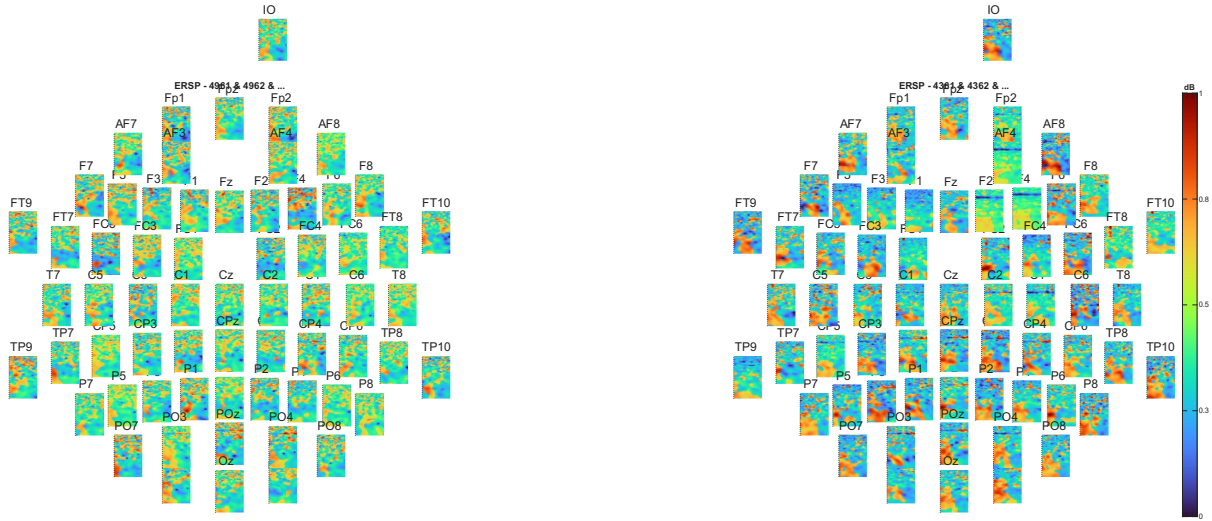


Figure 16: Time-frequency maps (ERSPs) for all channels, plotted separately for face and dollhouse stimuli.

To better interpret the differences between conditions, I further analyzed selected channels individually. The comparison plots below illustrate distinct oscillatory patterns for face vs. dollhouse stimuli.

Channel O1

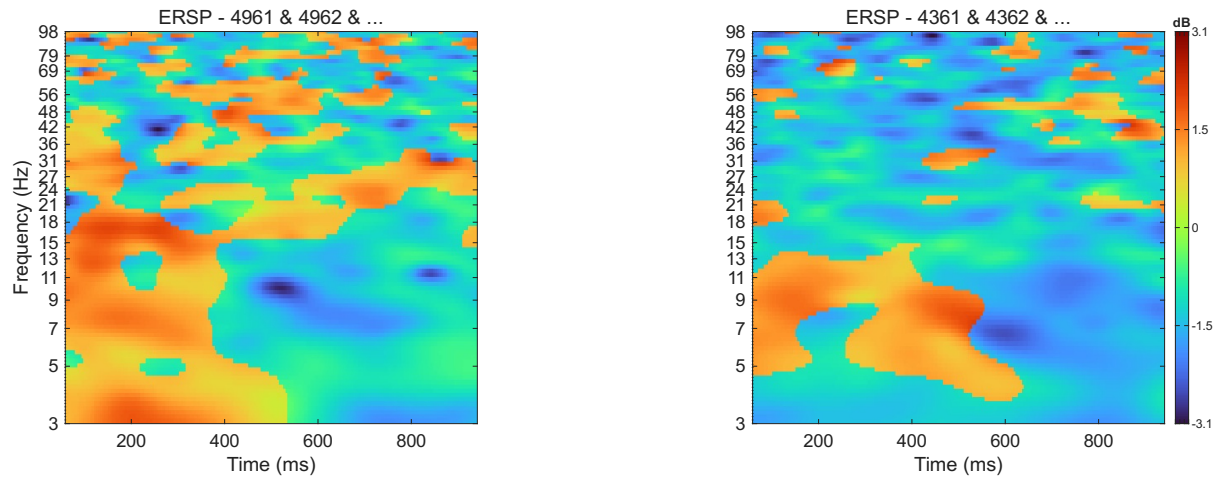


Figure 17: ERSP in channel O1: face vs. dollhouse.

In channel **O1**, face stimuli evoked a stronger increase in power in the **beta band (13–21 Hz)** around **200 ms** post-stimulus. A less pronounced but still noticeable increase was observed in the **theta to low alpha range (3–13 Hz)** in the same time window. These early occipital responses suggest enhanced visual processing for faces.

Channel PO4

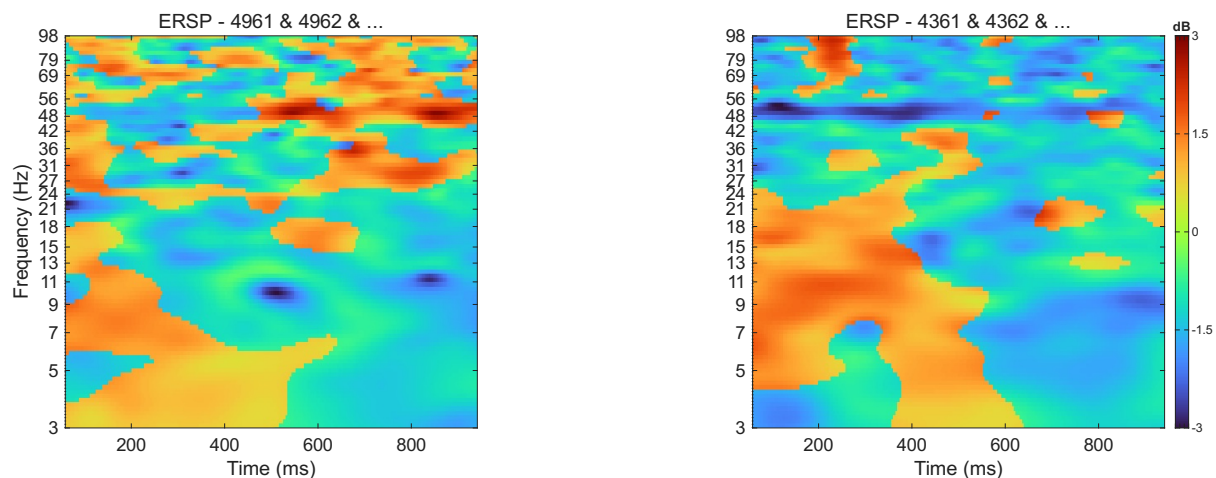


Figure 18: ERSP in channel PO4: face vs. dollhouse.

In channel **PO4**, a strong increase in **high gamma activity (30–80 Hz)** was observed between **600–800 ms** following face stimuli. High gamma activity is often associated with local cortical processing and object recognition, indicating increased cognitive demands during face perception.

Channel PO7

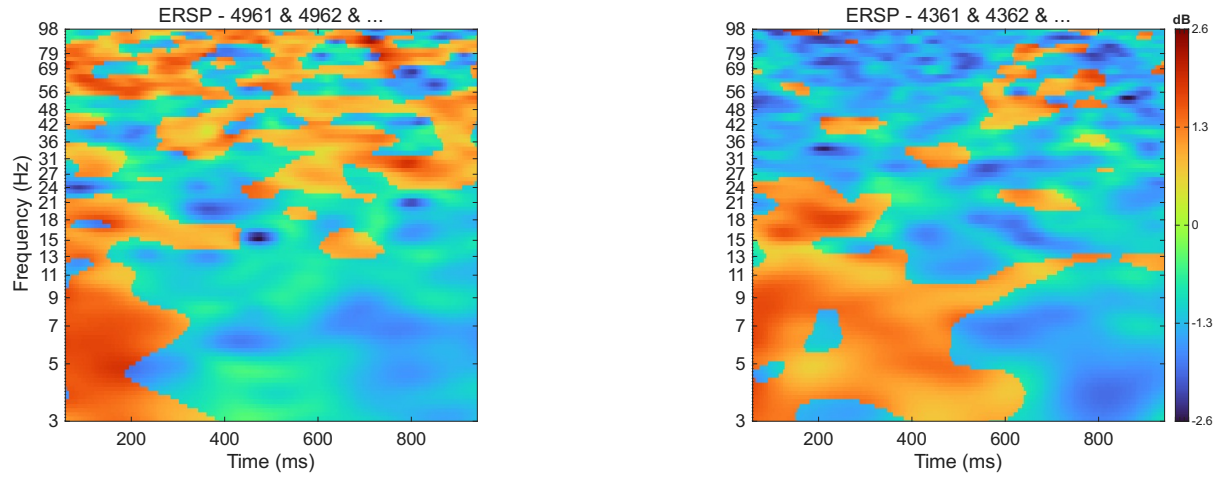


Figure 19: ERSP in channel PO7: face vs. dollhouse.

In channel **PO7**, face stimuli elicited enhanced **low-frequency activity (2–10 Hz)** between **100–200 ms**, consistent with theta and early alpha activity. Additionally, there were broad increases in **gamma activity (30–100 Hz)** throughout the trial duration. These oscillations may reflect both early perceptual encoding and sustained cognitive engagement with face stimuli.

Channel TP9

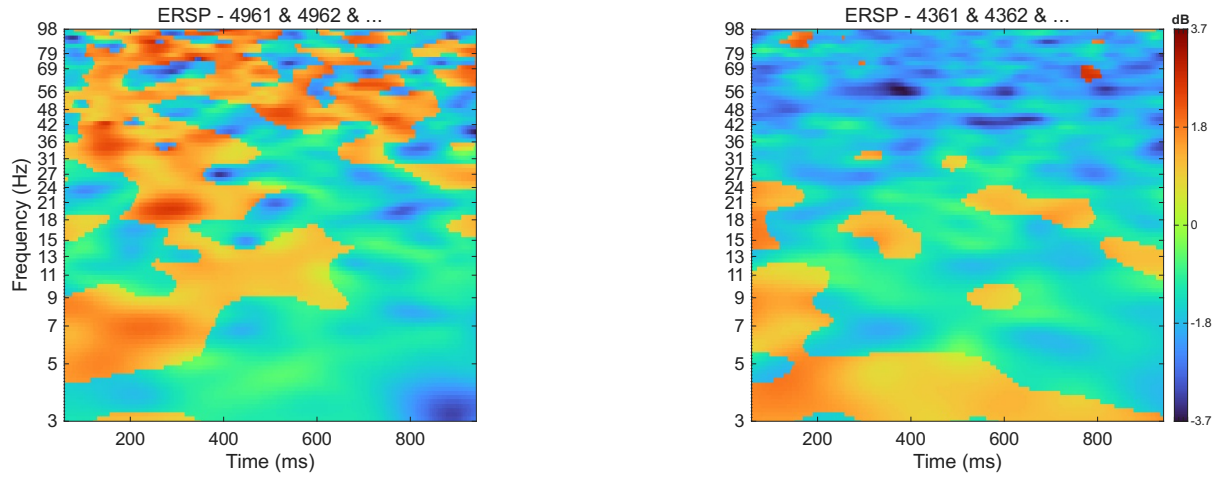


Figure 20: ERSP in channel TP9: face vs. dollhouse.

Channel **TP9** showed robust increases in **gamma-band power (30–100 Hz)** throughout the trial for face stimuli. This sustained high-frequency activity could be linked to working memory or attentional mechanisms selectively engaged during face perception.

Discussion

These results reveal clear distinctions in the time-frequency domain between face and dollhouse stimuli. Specifically:

- **Theta and alpha oscillations (2–13 Hz)** appear to support early-stage perceptual encoding.
- **Beta activity (13–30 Hz)** is enhanced during mid-latency face processing, potentially linked to higher-order visual integration.
- **Gamma oscillations (30–100 Hz)** are more prominent during face trials, especially in posterior and temporal electrodes, reflecting object recognition, attention, and higher-order cognitive processing.

Overall, the time-frequency analysis supports the idea that faces engage both early visual areas and higher-level temporal-parietal regions, with distinct patterns across frequency bands.

Multivariate Pattern Analysis (MVPA)

To explore whether EEG patterns can distinguish between face and dollhouse stimuli, I conducted multivariate pattern analysis (MVPA) using the MVPA-Light toolbox. I applied both temporal and spatial decoding, as well as cross-temporal generalization.

4.1 Temporal MVPA

I trained a linear discriminant analysis (LDA) classifier at each time point to classify face vs. dollhouse trials. A 5-fold cross-validation scheme was used to evaluate classification performance. The results are presented below in terms of accuracy, AUC (area under the ROC curve), and F1 score:

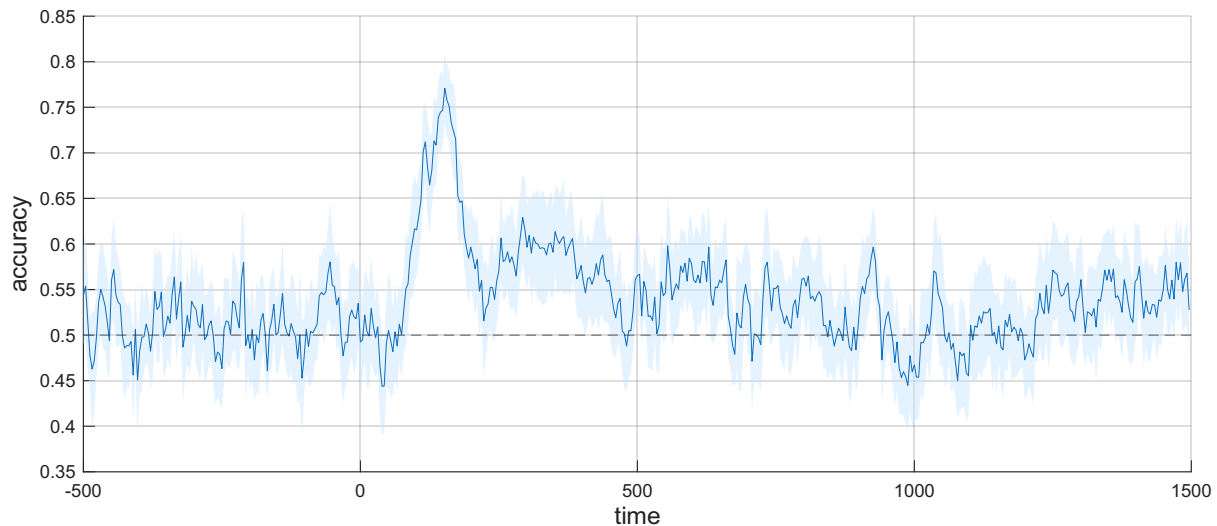


Figure 21: Temporal decoding accuracy over time.

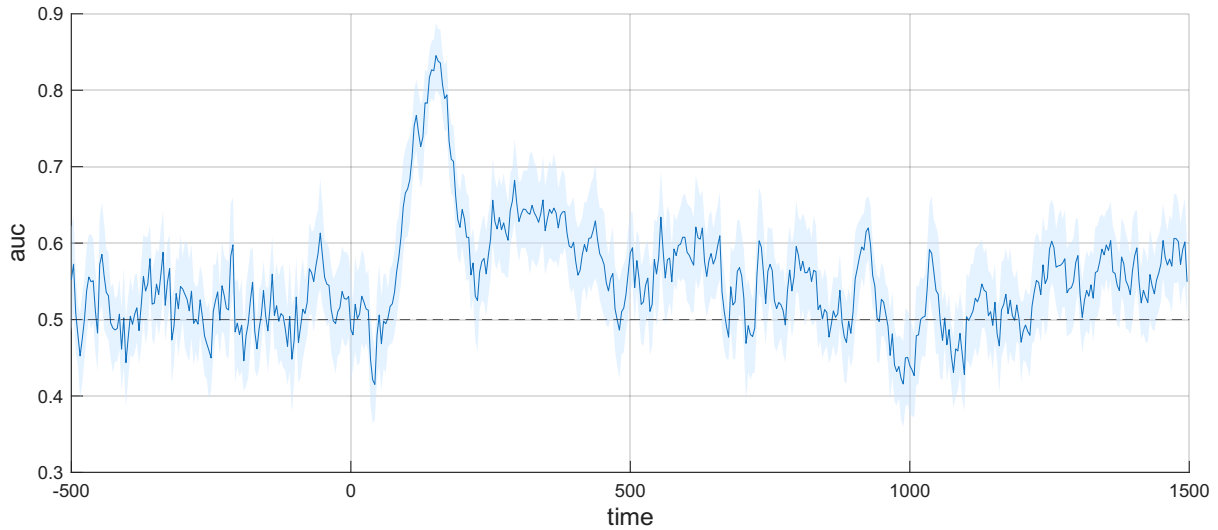


Figure 22: Temporal decoding AUC score over time.

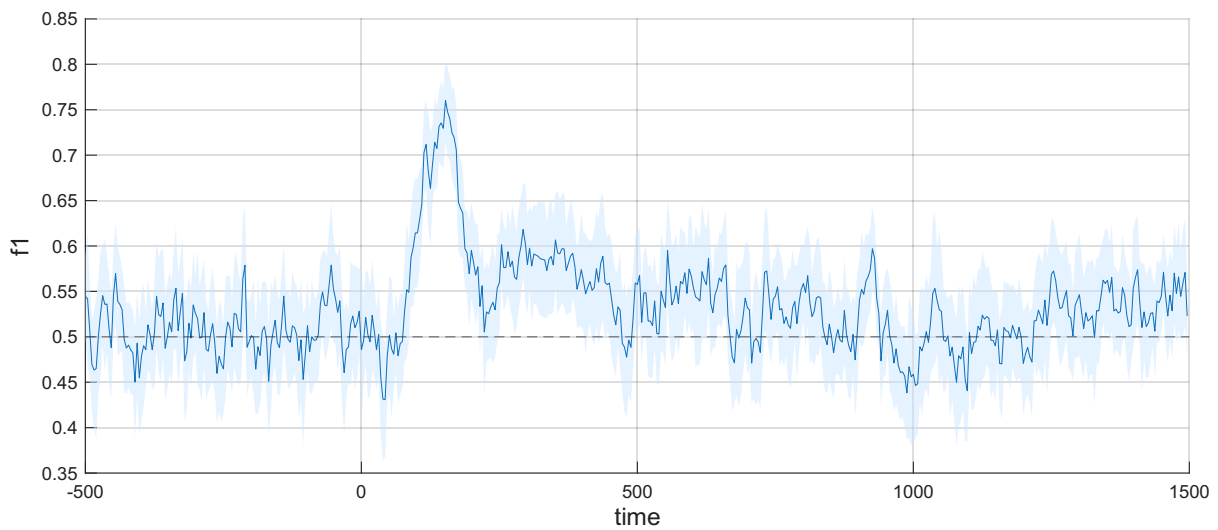


Figure 23: Temporal decoding F1 score over time.

All three metrics show a distinct peak around **170 ms post-stimulus**, reaching values close to 0.8. This suggests that face and dollhouse stimuli can be reliably distinguished using EEG activity at this latency, consistent with the N170 ERP component known to be sensitive to face perception. Therefore, the time window of **150–200 ms** is especially informative for distinguishing between the two categories.

4.2 Spatial MVPA

To examine spatial patterns, I averaged the EEG signals from **100 to 300 ms** post-stimulus and trained an LDA classifier using the spatial distribution of EEG activity across all channels. To visualize the spatial contributions, I plotted a topographical map of the classifier weights:

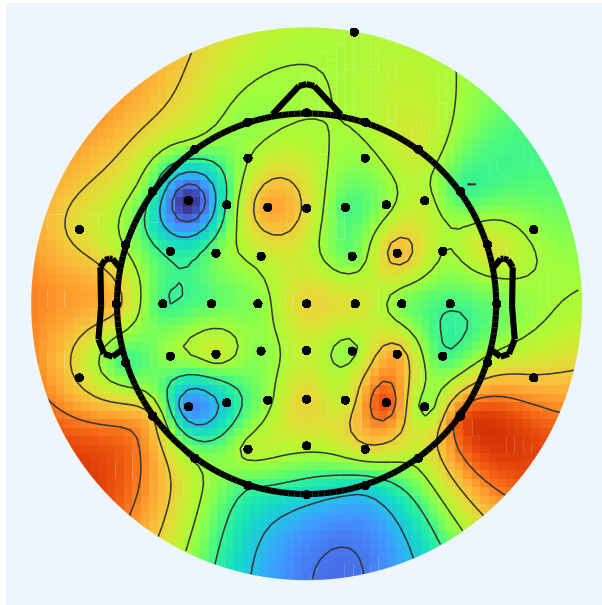


Figure 24: Topographic map of LDA classifier weights during 100–300 ms.

As shown, the weights are highest in the **posterior electrodes P7 and P8**, suggesting that these regions contribute most to discriminating between face and dollhouse trials. These areas are consistent with known occipito-temporal regions involved in face processing, supporting the spatial selectivity of the decoding model.

4.3 Cross-Temporal Generalization

Finally, I computed a time-by-time generalization matrix by training the LDA classifier at one time point and testing it across all others. This method allows us to assess the temporal stability and evolution of stimulus-related neural representations.

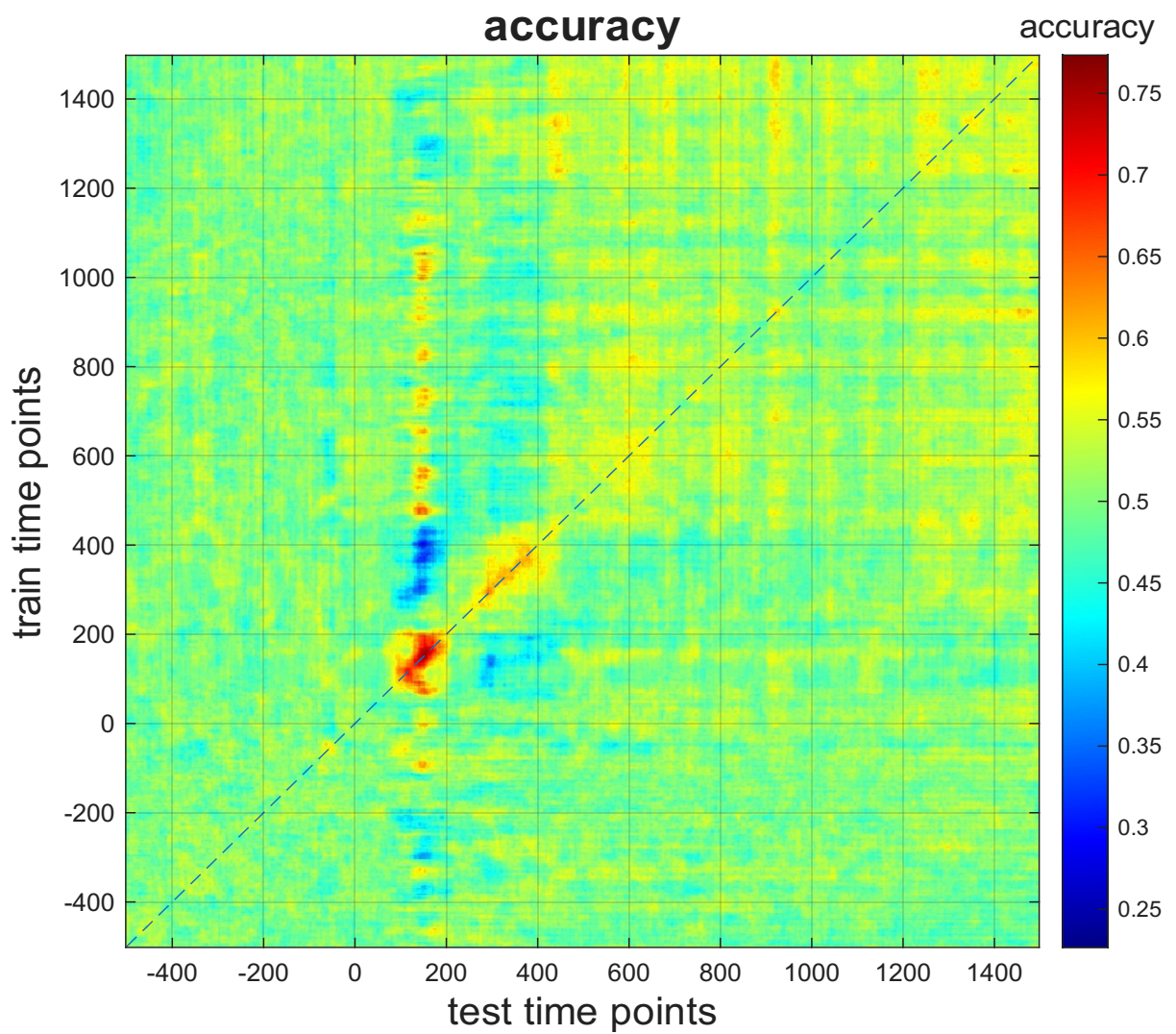


Figure 25: Cross-temporal generalization matrix (accuracy).

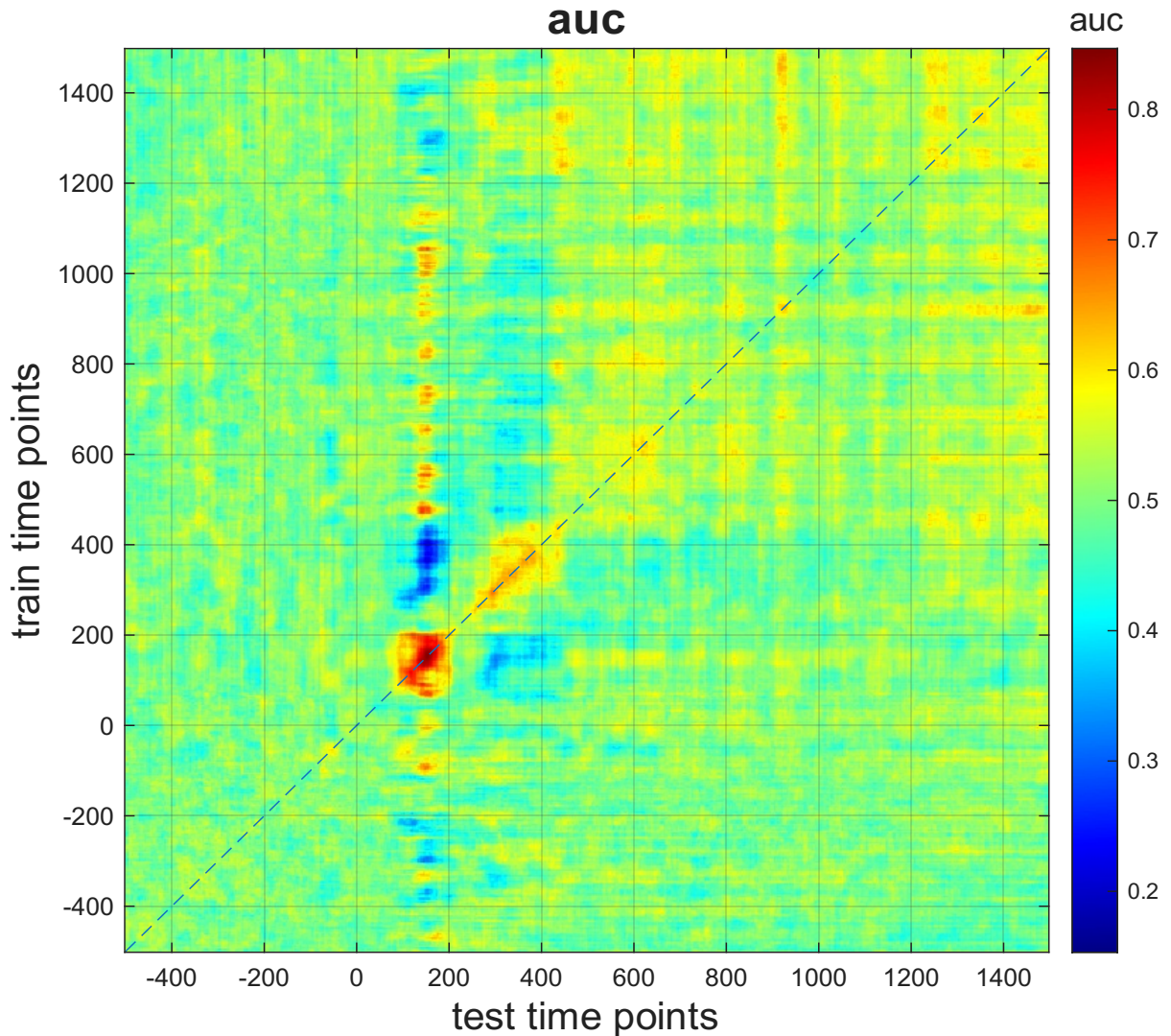


Figure 26: Cross-temporal generalization matrix (AUC).

The diagonal of the matrix shows high decoding performance around **170 ms**, again confirming this as a critical time point. Furthermore, the surrounding off-diagonal areas also show elevated classification performance, indicating that the neural representations are stable over a short temporal window.

In addition, a second region of elevated decoding appears around **300–400 ms**, suggesting the emergence of a later, possibly more abstract, stage of stimulus processing. This could reflect higher-level categorization or decision-related activity, consistent with the P300 ERP component.

Interpretation

- EEG signals contain reliable patterns that distinguish face and dollhouse stimuli, particularly around 170 ms after stimulus onset.
- Posterior channels (especially P7 and P8) contribute most to this distinction, aligning with known face-sensitive regions.
- The time-by-time generalization analysis reveals both early and late stages of category-selective processing, indicating dynamic and evolving neural representations in time.

These findings reinforce the notion that object processing in the brain involves temporally distinct and spatially localized neural dynamics, with early signals reflecting perceptual encoding and later activity supporting categorization and decision-making.

Representational Dissimilarity Matrices (RDM) and Representational Similarity Analysis (RSA)

To explore the structure of neural representations in response to visual stimuli, I computed Representational Dissimilarity Matrices (RDMs) from both EEG and deep neural network activations. The RDMs capture how distinct the neural patterns are across different stimuli.

EEG RDMs: Across Time and Channels

First, I computed EEG-based RDMs across time and channels.

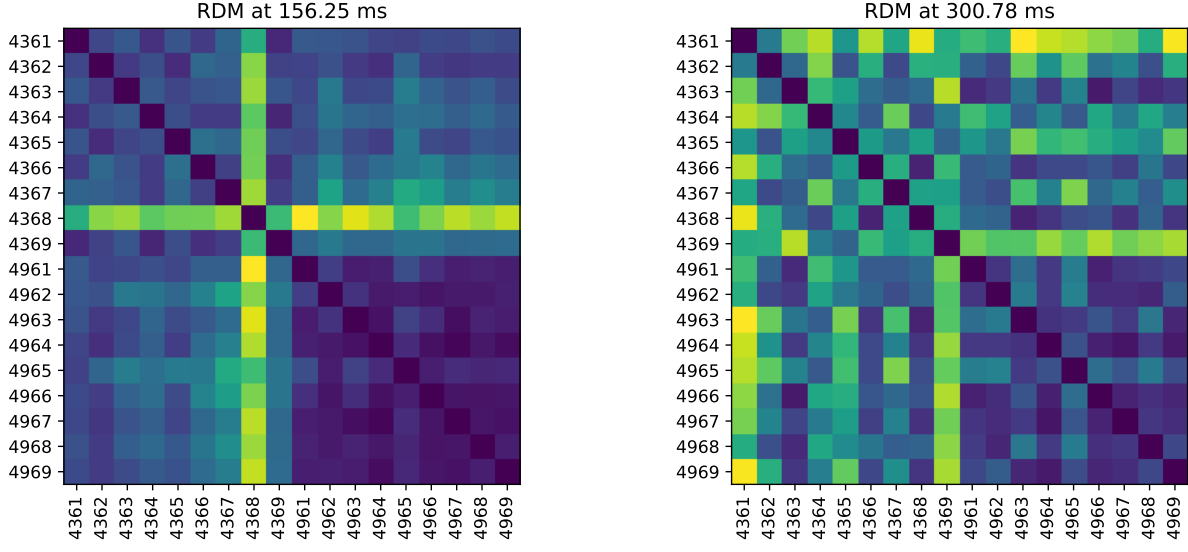


Figure 27: EEG RDMs over time.

As shown above, the dissimilarity between EEG responses to different face stimuli sharply decreases around **156 ms**, indicating that neural activity becomes more consistent across face exemplars. This timing coincides with the known N170 component, which is commonly associated with face-specific processing.

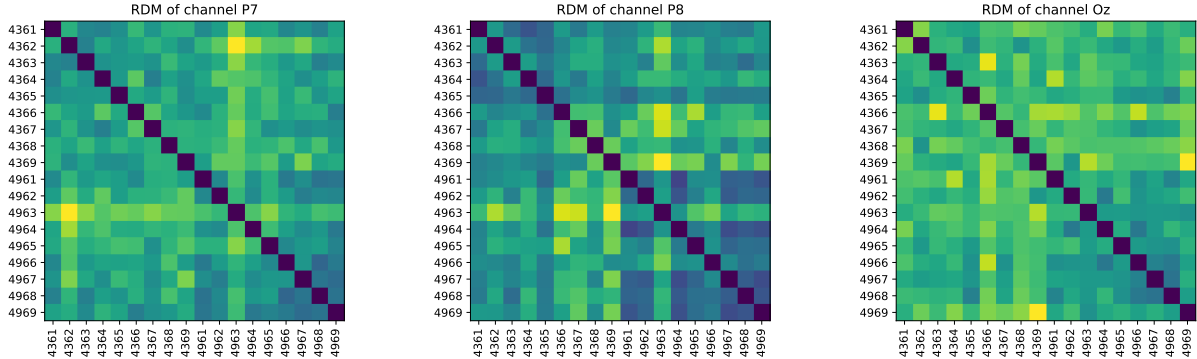


Figure 28: EEG RDMs across channels.

In the spatial domain, channel-wise RDMs revealed that **P8** exhibits the highest similarity across face stimuli, with somewhat similar trends also observed in **P7** and **Oz**. These channels are located in posterior scalp regions, consistent with occipito-temporal involvement in visual object perception.

Deep Neural Network Features (CORnet-S)

To compare EEG representations with hierarchical visual representations in a brain-inspired model, I extracted features from the CORnet-S model at four layers: **V1, V2, V4, and IT**. These layers simulate the progression of visual processing in the ventral stream.

RSA: EEG vs. CORnet-S

I computed the Representational Similarity Analysis (RSA) by correlating the EEG RDMs over time with the RDMs from CORnet-S layers.

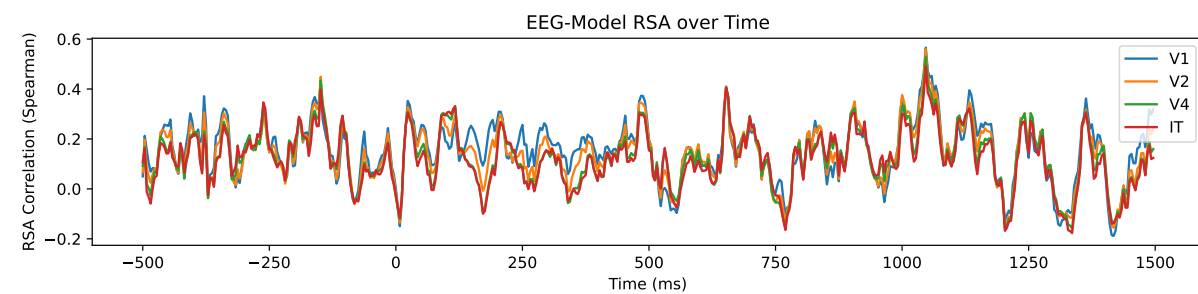


Figure 29: RSA over time between EEG and CORnet-S RDMs (V1, V2, V4, IT).

The plot shows that:

- The EEG RDMs correlate most strongly with early CORnet-S layers, particularly **V1**, followed by **V2**.
- These correlations peak between approximately **130 ms and 370 ms**, a time window that aligns with early visual and object-related processing in the brain.
- Higher layers such as **V4** and **IT** show lower RSA scores, suggesting that EEG primarily captures lower-to-mid-level visual representations in this task.

Interpretation and Hypotheses

- **Do some visual layers of CORnet-S correlate more with EEG activity than others?**
Yes — the RSA results show that **V1 and V2 layers correlate significantly more** with

EEG RDMs than V4 and IT, indicating that early visual features are more strongly reflected in the scalp EEG signals.

- **Can you identify temporal dynamics that resemble ventral stream processing?** Indeed, the time-resolved RSA reveals a progression that mirrors ventral stream dynamics: early EEG time points correlate more with V1 and V2, suggesting initial feature encoding, followed by lower correlation with deeper layers, possibly due to EEG's reduced sensitivity to high-level abstract representations like those in IT.
- **Discuss any hypotheses and provide supporting evidence.** Our hypothesis was that early EEG signals (~150–250 ms) would align with early visual cortex representations (V1/V2), while later stages might reflect more abstract processing. This was supported by the RSA curves, which peaked in the **150–300 ms** range, especially for **V1**, and by the fact that early occipital electrodes (e.g., P8, Oz) showed higher representational similarity for face stimuli. These findings suggest that EEG captures hierarchical visual information in a way that partially mirrors the ventral stream's progression from low-level to mid-level processing.

Conclusion

The RSA analysis supports the notion that scalp EEG contains meaningful representational structure related to early visual processing, particularly for faces. While deeper cortical processing (as modeled by CORnet-S layers V4 and IT) may not be fully reflected in scalp-level EEG, the alignment with V1 and V2 layers reinforces the idea that early EEG activity is dominated by low-level feature encoding.